Eur Radiol (2004) 14:1949–1955
DOI 10.1007/s00330-004-2445-7

A.-J. Lemke
M.-I. Senfft von Pilsach
A. Lübbe
C. Bergemann
H. Riess
R. Felix

MRI after magnetic drug targeting in patients with advanced solid malignant tumors

Received: 12 December 2003
Revised: 2 July 2004
Accepted: 8 July 2004
Published online: 5 August 2004

The used data are part of the thesis of M.-I. Senfft von Pilsach.

A.-J. Lemke (✉) · M.-I. Senfft von Pilsach
R. Felix
Universitätsklinikum Charité,
Campus Virchow-Klinikum,
Medizinische Fakultät
der Humboldt-Universität zu Berlin,
Klinik für Strahlenheilkunde,
Berlin, Germany
e-mail: lemke@charite.de
Tel.: +49-30-450557001
Fax: +49-30-450557901

A. Lübbe
Cecilien-Klinik,
Bad Lippspringe, Germany

C. Bergemann
Chemicell GmbH,
Berlin, Germany

H. Riess
Universitätsklinikum Charité,
Campus Virchow-Klinikum,
Medizinische Fakultät
der Humboldt-Universität zu Berlin,
Medizinische Klinik,
Schwerpunkt Hämatologie und Onkologie,
Berlin, Germany

Abstract The purpose of this study was to evaluate the ability of MRI to detect magnetic particle uptake into advanced solid malignant tumors and to document the extension of these tumors, carried out in the context of magnetic drug targeting. In a prospective phase I trial, 11 patients were examined with MRI before and after magnetic drug targeting. The sequence protocol included T1-WI and T2-WI in several planes, followed by quantitative and qualitative evaluation of the signal intensities and tumor extensions. In nine patients, a signal decrease was observed in the early follow-up (2–7 days after therapy) on the T2-weighted images; two patients did not show a signal change. The signal changes in T1-WI were less distinct. In late follow-up (4–6 weeks after therapy), signal within nine tumors reached their initially normal level on both T1-WI and T2-WI; two tumors showed a slight signal decrease on T2-WI and a slight signal increase on T1-WI. Within the surveillance period, tumor remission in 3 out of 11 patients was observed, and in 5 patients tumor growth had stopped. The remaining three patients showed significant tumor growth. There was no statistically significant correlation between signal change and response. MRI is a suitable method to detect magnetite particles, deposited at the tumor site via magnetic drug targeting. MRI is therefore eligible to control the success of MDT and to assess the tumor size after the end of therapy.

Keywords MRI · Magnetic drug targeting · Local chemotherapy · Magnetite-bounded epirubicin · Solid malignant tumors

Introduction

A long-standing wish of oncological therapy is to treat locally confined diseases locally and systemically spread diseases systemically. If local therapy (e.g., surgery) is inapplicable, a local disease has to be treated systemically, the treatment of the local disease therefore being associated with the toxic adverse effects of a generalized systemic distribution. So-called “drug targeting”, that is directing a drug as precisely as possible to the desired region, effectively mitigates harmful side effects and offers the possibility to apply a systemically lower dose [1].

Due to their relatively nonspecific action, chemotherapeutics have a tendency of toxicity to healthy tissue, even under optimal conditions. Being able to concentrate the drug in the tumor region, increasing anti-tumor efficacy with applying a locally higher but systemically lower dose would minimize this problem. Also positive economic aspects, e.g., having to use less amounts of the drug administered, can be taken into consideration.

Over the last 20 years, different approaches to drug targeting of chemotherapeutics have been pursued, mainly distinguishing between active and passive drug targeting. Active drug targeting combines specific tumor cell antibodies with anticancer drugs [2]; passive drug targeting binds a drug to a magnetic substance (ferrofluid) [1], which is directed into the desired region by an externally applied magnet (magnetic drug targeting, MDT). A remarkable attribute of ionically bound drugs to the surface of specific drug delivery systems is that the active low molecular weight substances can desorb from the carriers after a defined time span and can, thus, diffuse from the vascular wall into the tissue [3]. This approach has also been successfully tested in animal experiments [4].

MRI, an established method in iron-enhanced liver diagnostics, presents ideal characteristics [5] to supervise magnetic drug targeting, but the ability of MRI to detect small amounts of iron particles had to undergo further investigation. The purpose of the following study is to use MRI to survey the uptake of a drug-magnetite complex into the tumor and to assess the tumor size within a follow-up examination.

Materials and methods

In a prospective phase I clinical trial, 13 patients with unsuccessful conventionally pretreated malignant tumors were treated by magnetic drug targeting and examined with MRI. The study was approved by the local ethics committee, and all patients had to sign an informed consent. Two of the 13 patients were excluded from further evaluation because MR examination was done before drug targeting, but could not be continued in the follow-up procedure because of bad medical conditions in consequence of their specific diseases. The remaining group (11 patients) consisted of 8 women and 3 men, with a mean age of 51 years (15–73 years, median 55 years). The tumors of all 11 patients were located at various, but intentionally chosen superficial sites. Most frequent were recurrent thoracic wall carcinomata and metastasis of breast carcinomata (n=3), followed by two metastatic chondrosarcomata (axilla and thigh). There were single cases of one histiocytoma (inguinal), one sarcoma (shoulder), one cystosarcoma (breast), one Ewing sarcoma (shoulder), one recurrent adenocarcinoma (parotid gland) and one inflammatory breast carcinoma.

For the accomplishment of magnetic drug targeting, a number of permanent magnets (B–Fe–Nd magnet) were arranged above the target area with a frame attached to the patient's bed and in minimal distance (less than 0.5 cm) to the tumor. The combination of up to ten permanent magnets, size 8×4×2 cm or 3×3×1 cm, resulted in a total field intensity of at least 0.5 T and in general 0.8 T. After the placement of the magnets above the tumor, a compound of ferrofluid (Nano-Technologies GBR, Berlin, Germany) and bounded epirubicin (4′-epidoxorubicin; Farmorubicin) was injected i.v. over 15 min into a cubital vein located contralaterally to the tumor. The ferrofluid was a colloidal dispersion, made by wet chemical methods from iron oxides and hydroxides into special multidomain particles; magnetic particles with a mean size of 100 nm were used. On the basis of a reversible binding, the desorption of the drug took place according to the physiological environment (pH, osmolality) [4]. The patients remained in the same position for 60–120 min. In the course of the study, drug targeting was carried out with an increasing dose per unit time of chemotherapeutic agent (5–100 mg epirubicin/m^2 over a period of a minimum of 3 and a maximum of 6 weeks). The applied cumulative dose lay between 16 and 310 mg epirubicin (Table 1). The total iron quantity applied per therapy session in drug targeting ranged from 132 to 468 mg. Before and particularly after the injection of the magnetite-linked anticancer drugs, intensive lab controls (e.g., hemograms) were done, and the patients were clinically supervised (e.g., ECG, NIBP). The described therapy was repeated up to two times within the following 2 weeks.

The initial MR examination of the tumor region was done 1–2 weeks before the start of the therapy. After magnetic drug targeting, further MR imaging was performed as early follow-up (2–7 days after therapy) and late follow-up (4–6 weeks after therapy) after the treatment. MR images were obtained on a 1.5-T superconductive system (Magnetom SP63, Siemens AG, Erlangen, Germany) using the body coil or, if possible from an anatomical point of view, surface coils. Both, T1-WI and T2-WI sequences were used, in the transverse plane as well as in a tumor-adapted slice orientation. The following parameters were used:

Table 1 Age and diagnosis of the patients, localization of the tumor and applied doses

No.	Age	Diagnosis	Localization of the tumor	Epirubicin (mg/m^2)	Epirubicin total (mg)	Ferrofluid (ml)
01	19	Histiocytoma	Left inguinal	5	20	48
02	30	Sarcoma	Right shoulder	5	16	48
03	52	Cystosarcoma	Right breast	5	18	52
04	68	Breast carcinoma	Thoracic wall (relapse)	50	160	50
05	73	Chondrosarcoma	Right thigh	50	150	48
06	15	Ewing sarcoma	Left shoulder	50	310	78
07	56	Adenocarcinoma	Left parotid gland (relapse)	50	170	48
08	58	Breast carcinoma	Thoracic wall (relapse)	75	280	52
09	55	Inflammatory carcinoma	Right breast	75	250	52
10	68	Breast carcinoma	Left upper arm (metastasis)	75	260	52
11	65	Chondrosarcoma	Right shoulder	100	200	25

– T1-WI: TR 610 ms, TE 14 ms, 3 acquisitions, FOV 230 mm, matrix 256×256 pixel, slice thickness 6 mm, examination time 4:34 min
– T2-WI: TR 4,600 ms, TE 90 ms, 2 acquisitions, FOV 230 mm, matrix 256×256 pixel, slice thickness 6 mm, examination time 6:20 min

For the analysis of the MR examination, the extension of the tumor was determined by three representative diameters. Following the RECIST criteria, partial response (PR) was defined as at least a 30% decrease of the largest diameter of the tumor; progressive disease (PD) was defined as at least a 20% increase of the largest diameter of the tumor. Stable disease (SD) was defined as neither sufficient shrinkage to qualify for PR nor sufficient increase to qualify for PD. The signal intensities were specified inside the tumor and in comparable healthy muscle tissue and put in proportion to each other to obtain the relative signal intensities for intraindividual and interindividual comparison. As far as possible in the examined area, the signal intensities of the liver were also documented. The evaluation was performed in consensus by three board-certified radiologists experienced in MRI of the musculoskeletal system on the base of hardcopy films.

Results

Overall, the tolerance of magnetic drug targeting was very good; only one patient did not tolerate the supine position—because of discomfort created by the tumor location—over the whole period of MR examination time, so that the procedure had to be interrupted only once for a brief time. Neither typical adverse effects (e.g., back pain, chest pain, sensation of heat), as they sometimes occur when ferrous contrast agents are applied, nor changes in the clinical-chemical parameters were observed.

In eight patients, the signal in the liver could also be evaluated because of their topographical proximity to the tumor. Especially in the early follow-up (up to 7 days post MDT), clear signal decreases in the liver were observed in eight patients over time, particularly in T1-WI. The decreased signals on T1-WI were still detectable to a minor degree in five patients in the late follow-up (4–6 weeks after therapy). In three patients, the liver signal corresponded with the signal before MDT on T1-WI (Fig. 1). On T2-WI, the effect was less distinct; here, slight signal decreases appeared in seven patients in the early follow-up, and in one patient no signal change was observed. The signals on T2-WI reached a normal level within 4–6 weeks in six patients; two patients still showed signal decrease in the liver in the late follow-up (Table 2).

In the early follow-up after the end of the therapy, 9 out of 11 patients showed a decreased signal in T2-WI within the tumor; out of these 9 patients, one case showed a strong signal decrease and one other case a strongly inhomogeneous signal decrease in the tumor. Only two tumors did not show a signal decrease after MDT. In the late follow-up exam, in 9 out of 11 patients, the signal reached a normal level, and 2 still showed marginal residual signal decreases (Fig. 2). In T1-WI, a very diverse signal behavior was observed after MDT. In the first follow-up exam, a strong inhomogeneous signal increase was observed in two patients, two showed a moderate signal increase, and seven tumors did not present a signal change (n=6) or only a slight signal decrease (n=1). In the late follow-up exam, the signal from within the tumor reverted to its initial state in nine tumors; only the two tumors with a primary strong signal increase still featured an increased signal (Table 3).

Within the surveillance period partial tumor response (PR) was observed in 3 out of 11 patients (Fig. 3) and stable disease (SD) in 5 patients. The remaining three patients showed progressive disease (PD).

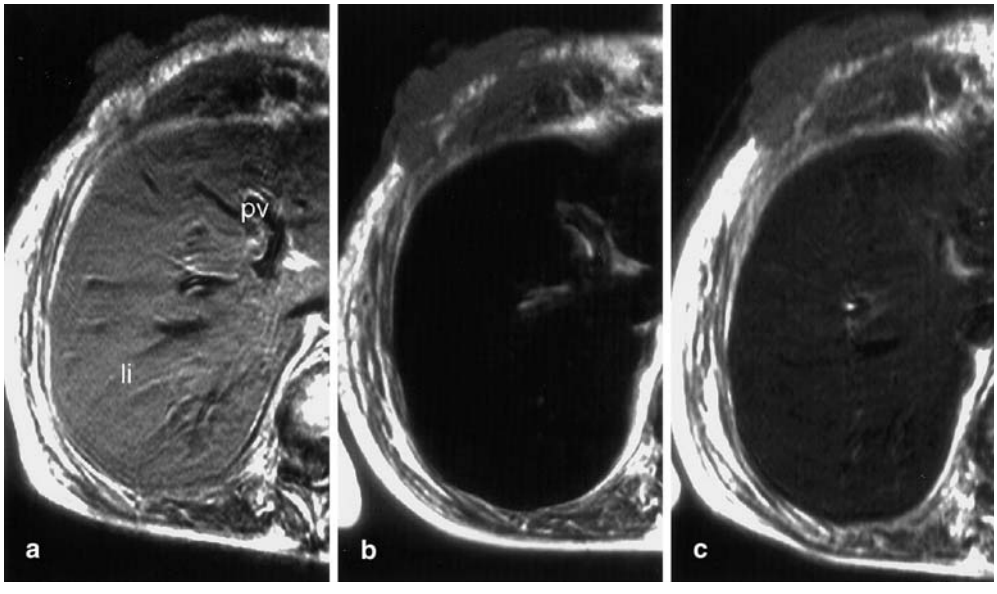

Fig. 1 Progression of signal intensities in the liver within 4 weeks after magnetic drug targeting on T1-WI. TR 610 ms, TE 14 ms, three acquisitions, FOV 230 mm, matrix 256×256 pixel, slice thickness 6 mm (*li* liver, *pv* portal vein branch). **a** Normal signals in the liver before the beginning of therapy with normal contrast between liver parenchyma and liver vessels (T1-WI). **b** Clear signal decrease in the liver 3 days after MDT nearly totally nullified contrast between liver parenchyma and liver vessels. **c** Also 4 weeks after MDT reduced signal in the liver

Table 2 Signal changes in the liver in comparison to examination before MDT (⇊ strong signal decrease, ↓ moderate signal decrease, = no signal change, *n.a.* not available)

No.	T1-WI		T2-WI	
	Early follow-up after MDT (2–10 days)	Late follow-up after MDT (4–6 weeks)	Early follow-up after MDT (2–10 days)	Late follow-up after MDT (4–6 weeks)
01	⇊	=	↓	=
02	⇊	↓	↓	=
03	⇊	↓	↓	↓
04	⇊	=	↓	=
05	n.a.	n.a.	n.a.	n.a.
06	n.a.	n.a.	n.a.	n.a.
07	n.a.	n.a.	n.a.	n.a.
08	⇊	↓	↓	↓
09	⇊	↓	=	=
10	⇊	=	↓	=
11	⇊	↓	↓	=

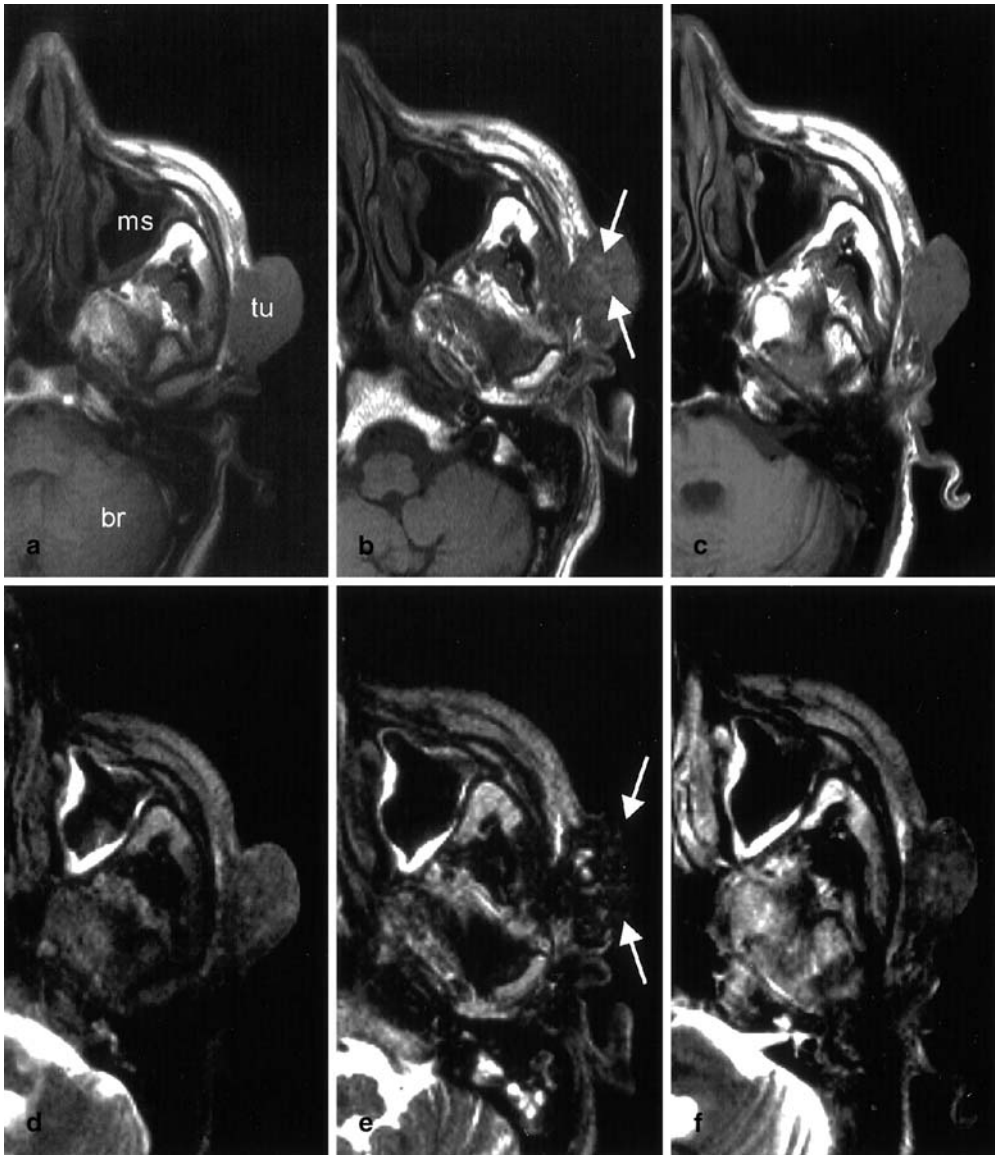

Fig. 2 Signal course after MDT in a 56-year-old patient with adenocarcinoma of the parotid gland before as well as 8 days and 6 weeks after MDT (**a–c** T1-WI, **d–f** T2-WI). T1-WI: TR 610 ms, TE 14 ms, three acquisitions, FOV 230 mm, matrix 256×256 pixel, slice thickness 6 mm. T2-WI: TR 4600 ms, TE 90 ms, two acquisitions, FOV 230 mm, matrix 256×256 pixel, slice thickness 6 mm (*ms*, maxillary siuns; *br*, brain; *tu* tumor). **a** Before MDT, isointense signal intensities of the tumor in comparison to the brain parenchyma. **b** Inhomogeneous, hyperintense signals (*arrows*) inside the tumor 8 days after MDT. **c** After 6 weeks after MDT, signal intensities correspond to the initial diagnostic finding, tumor shows a partial regression. **d** Low signal intensities in the initial diagnostic finding. **e** Eight days after MDT slight signal decrease inside the tumor (*arrows*). **f** Signals reverse to initial state 6 weeks after MDT

Table 3 Signal changes in the tumor compared to examination before MDT (⇑ strong signal increase, ↑ moderate signal increase, = no signal change, ⇓ strong signal decrease, ↓ moderate signal decrease, *PR* partial response, *PD* progressive disease, *SD* stable disease)

No.	T1-WI		T2-WI		Tumor size
	Early follow-up after MDT (2–10 days)	Late follow-up after MDT (4–6 weeks)	Early follow-up after MDT (2–10 days)	Late follow-up after MDT (4–6 weeks)	
01	⇑ (inhomogenous)	↑	↓	=	SD
02	=	=	↓ (inhomogenous)	=	PR
03	↑	=	↓	=	PD
04	↓	=	↓	=	PR
05	=	=	↓	=	SD
06	↑	=	↓	↓	PD
07	⇑ (inhomogenous)	↑	⇓	↓	PR
08	=	=	↓	=	SD
09	=	=	=	=	SD
10	=	=	=	=	SD
11	=	=	↓	=	PD

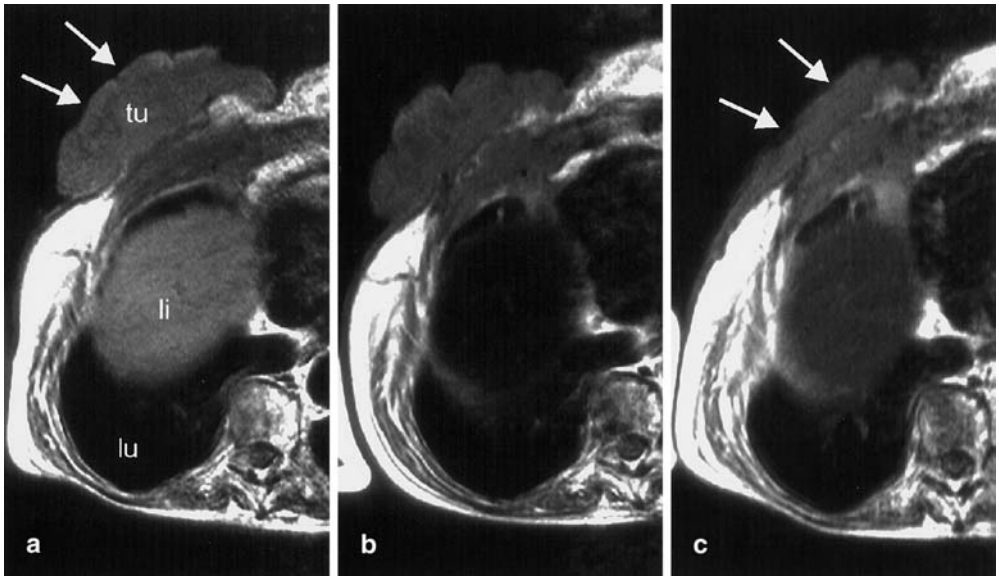

Fig. 3 Clear tumor regression in a 68-year-old patient with a thorax wall relapse of a mamma-carcinoma after magnetic drug targeting (T1-WI). T1-WI: TR 610 ms, TE 14 ms, three acquisitions, FOV 230 mm, matrix 256×256 pixel, slice thickness 6 mm (*li* liver; *lu* lung; *tu* tumor). **a** Before the beginning of therapy, exophytic tumor (*arrows*) on the right thorax wall at the border to the abdomen, normal signal in the liver, tumor slightly hypointense in comparison to the liver. **b** Contrast reversal between liver and tumor 2 days after MDT because of a strong signal decrease in the liver. Also a signal reduction of the tumor because of MDT. **c** Four weeks after the end of therapy still reduced signals in the liver next to normal signals in the markedly regressed tumor (*arrows*)

Two of eight patients with partial response or stable disease had a strong signal increase within the tumor in the early follow-up on T1-WI, and both tumors presented inhomogeneous enhancement. An inhomogeneous signal decrease was also seen in the early follow-up in one patient with partial regression. All other changes of the signal behavior within the tumors was seen in patients with progressive disease, stable disease and partial regression.

Discussion

In MRI, iron-compounds in various sizes have gained an important position within diagnostic investigation of the liver [6, 7] as well as of the spleen and lymph nodes [8, 9]. The addition of ferrumoxides showed an increase of sensitivity and specificity of hepatic MR evaluation compared to unenhanced MRI [10]. The specific accumulation in these organs can result in signal changes in healthy tissue so that tumorous tissue becomes clearly visible [11]. Magnetite particles also serve as carrier molecules for hormones, antibodies, radioactive markers or anticancer-drugs [12, 13]. In this case, these characteristics of magnetite particles can be used for controlling the magnetic anti-cancer drug complex from the out-

side [14] and, above all, MRI can locate these particles. Promising results of recent studies on ultrasmall superparamagnetic iron oxides (USPIOs, <50 nm) and superparamagnetic iron oxides (SPIOs, >50 nm) emphasize the possibilities that lie within this approach [15]. In this study SPIOs came into use.

The polymeric composition (e.g., hydrophobity, biodegradation profile) of both the nanoparticles and the associated drug (molecular weight, charge) has a major influence on the drug distribution pattern by the MPS (mononuclear phagocytes system) [16]. Based on this characteristic, it has been demonstrated that negatively charged and neutral particles stay for the longest time in the blood circulation before they are eliminated mainly by the reticuloendothelial system [17]. The targeting effectiveness for certain anatomical regions can be optimized through surface modification using biologically active substances such as antibodies or receptor ligands [18]. In order to reduce oponization reactions and to subsequent clearance by macrophages, the curvature (size <100 nm) and the hydrophilic surface are taken into consideration. It is very likely that after their dissociation from the drug, exogenous magnetite particles also enter the endogenic iron reserves (hematopoiesis) of the body [19].

Because of their superparamagnetic features, iron compounds enhance T1 and T2/T2* relaxation, but also show the ability to reduce the T2/T2* relaxation time [20]. All iron oxides lead to a signal decrease of benign lesions with either phagocytic cells or a significant blood pool on T2-weighted accumulation phase images. The signal decrease of benign lesions is commensurate to the Kupffer cell activity or tumor vascularisation and is useful for lesion characterization [21]. USPIOs have longer circulating properties than SPIOs and show a higher uptake by macrophages into the healthy parts of the lymph node [5]. This offers a novel clinical investigation method of the lymph node due to the fact that USPIOs lead to a signal decrease in the entire lymph node, while pathologic parts show no signal change [22].

In early follow-up, clear extinction phenomena were observed in the liver and spleen. This result may be surprising as—because of drug targeting— the complex should be localized primarily in the tumor region. The dissociation process (drug—magnetic particle) takes up to 30 min [4]. The drug is therefore released from the carrier substance, unfolds its effect locally and the nanoparticles are cleared by the MPS. Despite that fact, human tumor cells accumulate intracellularely up to 1 pg iron/cell, in the past demonstrated by electron microscope (TEM), X-ray spectroscopy and measurements of the intracellular iron [23]. The rapid extravasation and cellular uptake of the magnetic particles explain the fast tumor toxicity, the success depending on a good vascularisation of the tumor and also on the distance of the externally applied magnetic field. A supporting fact is that magnetic fluids show hyperthermia potential [24], which can lead to a better vascularisation. This characteristic could not only be used in tumors, but also in non-invasive thrombolysis of fine capillaries [18].

The T2 relaxitivity is more dependent on the magnetic susceptibility than on the iron percentage inside the particles [25]. For this reason, the use of more sensitive sequences (susceptibility measurements) could be taken into consideration. Such measurements are, compared to spin echo sequences, more vulnerable to artifacts, which can be problematic with seriously ill patients due to a lower compliance.Because of the fact that only superficially located tumors were chosen in this study, it will be necessary to exploit this field with other methods, e.g., insertation of a ferromagnetic wire into the vessels and placement in a strong magnetic field, herewith optimizing the depth range [26].

Although MRI was able to detect the iron particles in the liver, spleen and most of the examined tumors, there was no statistical relation between iron uptake in the tumor and the tumor control during the surveillance period. This may be due to the fact that the different tumor entities have different susceptibilities to anticancer drugs. In three cases with partial response or stable disease, inhomogenous signal changes on T1-WI or T2-WI were observed in the early follow-up, indicating a higher tumor vascularisation possibly helpful for the success of the treatment.

Furthermore, drug targeting holds the iron particles in the tumor region and postpones the systemic release—systemic adverse effects are reduced because of a slower inflow. The local effect allows the use of neoplastic agents, which would be too toxic for systemic use. The tolerance of magnetic drug targeting is very good, and MDT has proven to be a promising therapy approach for the treatment of superficially localized tumors. MRI is a suitable method to detect even small magnetite concentrations and is therefore eligible to control the storage of the iron-drug complex and to assess the tumor size after the end of therapy. Because of the small number of patients in this case, this method has to undergo further evaluation on a larger scale.

Acknowledgments This study was supported by the Graduiertenkolleg GRK 331 “Temperaturabhängige Effekte in Therapie und Diagnostik” of the German Research Foundation [Deutsche Forschungsgemeinschaft (DFG)].

References

1. Alexiou C, Jurgons R, Schmid RJ, Bergemann C, Henke J, Erhardt W, Huenges E, Parak F (2003) Magnetic drug targeting—biodistribution of the magnetic carrier and the chemotherapeutic agent mitoxantrone after locoregional cancer treatment. J Drug Target 11:139–149
2. Mamot C, Drummond DC, Greiser U, Hong K, Kirpotin DB, Marks JD, Park JW (2003) Epidermal growth factor receptor (EGFR)-targeted immunoliposomes mediate specific and efficient drug delivery to EGFR- and EGFRvIII-overexpressing tumor cells. Cancer Res 63:3154–3161
3. Chen Y, Mcculloch RK, Gray BN (1994) Synthesis of albumin-Dextran sulfate microspheres possessing favourable loading and release characteristics for the anticancer drug Doxorubicin. J Control Release 31:49–54
4. Lubbe AS, Bergemann C, Huhnt W, Fricke T, Riess H, Brock JW, Huhn D (1996) Preclinical experiences with magnetic drug targeting: tolerance and efficacy. Cancer Res 56:4694–4701
5. Bonnemain B (1998) Superparamagnetic agents in magnetic resonance imaging: physicochemical characteristics and clinical applications. A review. J Drug Target 6:167–174
6. Kumano S, Murakami T, Kim T, Hori M, Okada A, Sugiura T, Noguchi Y, Kawata S, Tomoda K, Nakamura H (2003) Using superparamagnetic iron oxide-enhanced MRI to differentiate metastatic hepatic tumors and nonsolid benign lesions. Am J Roentgenol 181:1335–1339
7. Reimer P, Balzer T (2003) Ferucarbotran (Resovist): a new clinically approved RES-specific contrast agent for contrast-enhanced MRI of the liver: properties, clinical development, and applications. Eur Radiol 13:1266–1276
8. Mack MG, Balzer JO, Straub R, Eichler K, Vogl TJ (2002) mSuperparamagnetic iron oxide-enhanced MR imaging of head and neck lymph nodes. Radiology 222:239–244
9. Sigal R, Vogl T, Casselman J, Moulin G, Veillon F, Hermans R, Dubrulle F, Viala J, Bosq J, Mack M, Depondt M, Mattelaer C, Petit P, Champsaur P, Riehm S, Dadashitazehozi Y, de Jaegere T, Marchal G, Chevalier D, Lemaitre L, Kubiak C, Helmberger R, Halimi P (2002) Lymph node metastases from head and neck squamous cell carcinoma: MR imaging with ultrasmall superparamagnetic iron oxide particles (Sinerem MR)—results of a phase-III multicenter clinical trial. Eur Radiol 12:1104–1113
10. Bluemke DA, Weber TM, Rubin D, de Lange EE, Semelka R, Redvanly RD, Chezmar J, Outwater E, Carlos R, Saini S, Holland GA, Mammone JF, Brown JJ, Milestone B, Javitt MC, Jacobs P (2003) Hepatic MR imaging with ferumoxides: multicenter study of safety and effectiveness of direct injection protocol. Radiology 228:457–464
11. Lee JM, Kim CS, Youk JH, Lee MS (2003) Characterization of focal liver lesions with superparamagnetic iron oxide-enhanced MR imaging: value of distributional phase T1-weighted imaging. Korean J Radiol 4:9–18
12. Elmi MM, Sarbolouki MN (2001) A simple method for preparation of immuno-magnetic liposomes. Int J Pharm 215:45–50
13. Alexiou C, Arnold W, Klein R, Parak F, Hulin P, Bergemann C, Erhardt W, Wagenpfeil S, Lubbe A (2002) Locoregional cancer treatment with magnetic drug targeting. Cancer Res 60:6641–6648
14. Lubbe AS, Alexiou C, Bergemann C (2001) Clinical applications of magnetic drug targeting. J Surg Res 95:200–206
15. Montet X, Lazeyras F, Howarth N, Mentha G, Rubbia-Brandt L, Becker CD, Vallee JP, Terrier F (2004) Specificity of SPIO particles for characterization of liver hemangiomas using MRI. Abdom Imaging 29:60–70
16. Couvreur P, Kante B, Lenaerts V, Scailteur V, Roland M, Speiser P (1980) Tissue distribution of antitumor drugs associated with polyalkylcyanoacrylate nanoparticles. J Pharm Sci 69:199–202
17. Weissleder R, Bogdanov A, Neuwelt EA, Papisov M (1995) Longcirculating iron oxides for MR imaging. Adv Drug Deliv Rev 16:321–334
18. Schutt W, Gruttner C, Hafeli U, Zborowski M, Teller J, Putzar H, Schumichen C (1997) Applications of magnetic targeting in diagnosis and therapy—possibilities and limitations: a mini-review. Hybridoma 16:109–117
19. Brigger I, Dubernet C, Couvreur P (2002) Nanoparticles in cancer therapy and diagnosis. Adv Drug Deliv Rev 54:631–651
20. Wang YX, Hussain SM, Krestin GP (2001) Superparamagnetic iron oxide contrast agents: physicochemical characteristics and applications in MR imaging. Eur Radiol 11:2319–2331
21. Reimer P, Tombach B (1998) Hepatic MRI with SPIO: detection and characterization of focal liver lesions. Eur Radiol 8:1198–1204
22. Schima W (2002) Organ specific MRI contrast media in general practice. Wien Med Wochenschr (Suppl) 113:8–11
23. Jordan A, Wust P, Scholz R, Tesche B, Fahling H, Mitrovics T, Vogl T, Cervos-Navarro J, Felix R (1996) Cellular uptake of magnetic fluid particles and their effects on human adenocarcinoma cells exposed to AC magnetic fields in vitro. Int J Hyperthermia 12:705–722
24. Jordan A, Scholz R, Wust P, Fahling H, Krause J, Wlodarczyk W, Sander B, Vogl T, Felix R (1997) Effects of magnetic fluid hyperthermia (MFH) on C3H mammary carcinoma in vivo. Int J Hyperthermia 13:587–605
25. Thomassen T, Wiggen UN, Gundersen HG, Fahlvik AK, Aune O, Klaveness J (1991) Structure activity relationship of magnetic particles as MR contrast agents. Magn Reson Imaging 9:255–258
26. Babincova M, Babinec P, Bergemann C (2001) High-gradient magnetic capture of ferrofluids: implications for drug targeting and tumor embolization. Z Naturforsch [C] 56:909–911